The Fermi surface of CeB_6

1996 J. Phys.: Condens. Matter 8 7105

(http://iopscience.iop.org/0953-8984/8/38/014)

J. Phys.: Condens. Matter **8** (1996) 7105–7125. Printed in the UK

The Fermi surface of CeB_6

M B Suvasini†, G Y Guo‡, W M Temmerman‡, G A Gehring† and M Biasini§‖

† Department of Physics, University of Sheffield, Sheffield S3 7RH, UK
‡ Daresbury Laboratory, Warrington WA4 4AD, UK
§ H H Wills Physics Laboratory, University of Bristol, Bristol BS8 1TL, UK

Received 15 May 1996

Abstract. The heavy-fermion compound CeB_6 has been studied using the fully relativistic spin-polarized mean muffin-tin orbital method within the local density approximation. Two separate calculations, one where the f electron is treated as a valence electron and the other where it is treated as part of the core, have been performed and the Fermi surface is obtained. The angular-dependent de Haas–van Alphen (dHvA) frequencies are calculated in both cases and they are compared with the experimental dHvA frequencies. We also calculated the electron momentum densities and compared them with the electron–positron momentum densities measured from the two-dimensional angular correlation of electron–positron annihilation radiation. The spin polarization of the Fermi surface is analysed and we present a new interpretation of the experimental data of Harrison *et al*.

1. Introduction

An important question in heavy-fermion physics is whether the f electron contribute to the Fermi surface. In UPt_3, the most thoroughly studied heavy-fermion system, the agreement of the de Haas–van Alphen (dHvA) frequencies obtained from a band calculation where f electrons are treated as valence electrons with the experimental results was a clear indication that the f electrons do contribute to the Fermi surface [1]. This is also true in the other U-based heavy-fermion system, UPd_2Al_3, where a satisfactory agreement is obtained between the experimental and the calculated dHvA frequencies [2]. In Ce compounds a clear picture has not emerged yet, particularly in the heavy-fermion compound CeB_6, which has been well studied using dHvA measurements [3–7] and with positron annihilation [8]. All these experiments seem to suggest that the f electron is almost localized. To shed some light on this important issue, we perform band structure calculations.

The Fermi surface of CeB_6 resembles closely that of LaB_6, a reference compound which has no f electron, suggesting the f electron might be localized. In other words, this seems to suggest that a band calculation which keeps the f electron as part of the core should reproduce the observed data. However the large mass enhancements in CeB_6 (specific heat coefficient, $\gamma = 250$ mJ mol^{-1} K^{-2} compared with the value of 2.6 mJ mol^{-1}K^{-2} in LaB_6) suggest that the f electrons in CeB_6 are itinerant rather than localized. This paper contains a detailed comparison between theory and experimental dHvA data and the electron–positron momentum density measured by two-dimensional angular correlation of electron–positron

‖ Permanent address: ENEA, via don Fiammelli 2, 40129 Bologna, Italy.

0953-8984/96/387105+21$19.50

annihilation radiation (2D ACAR), to address the issue of the localization of the f electron in CeB_6.

In this paper we use the two different models of a localized and a valence f electron to reinvestigate the Fermi surface of the heavy-fermion compound CeB_6. These calculations are an improvement over the previously reported band structure calculations [9] on CeB_6, in that we use a fully relativistic band structure method. Two separate calculations are performed, one where the f electron is treated as itinerant (f-band calculations) and the other where it is treated as part of the core (f-core calculations). Hereafter, we refer to these calculations as 'f band' and 'f core'. The Fermi surface is obtained from spin-polarized, ferromagnetic, f-band and f-core calculations and the dHvA frequencies and the momentum densities are calculated and compared with experiments.

It is a known fact that the simple local density approximation (LDA) employed in a band structure calculation is not adequate to treat strongly correlated systems. In heavy-fermion systems the effective mass is underestimated by a factor of 20 [10]. The LDA however has been successful with regards to *Fermi surface topology*, for instance in UPt_3 [9]. Recently we found that the metamagnetic transition of UPt_3 can also be explained within the LDA [11]. Thus one expects a reasonable model of the Fermi surface and ground state energies within the LDA.

CeB_6 undergoes two phase transitions, one at 3.2 K to the antiferroquadrupolar phase and the other at 2.3 K to the antiferromagnetic phase [12]. The dHvA experiments are performed in the antiferroquadrupolar phase. According to Norman and Koelling, non-magnetic f-core calculations give a better fit to the experiment [13]. The spin-polarized f-band calculations of Langford *et al* [9] on the other hand do not give a good quantitative agreement with experiments and a shift in E_F of more than 10 mRyd is needed to match the α frequency, while the other branches were not calculated. This calculation does not include spin–orbit coupling and this could prove to be important as the bands forming the Fermi surface have substantial f content. A fully relativistic and spin-polarized calculation however can determine the influence of the spin–orbit coupling on the spin polarization of the electron bands. A consequence is the spin is no longer a good quantum number and the electronic bands can be differently spin polarized. In particular, each of the Fermi surface sheets can have a different spin polarization.

In section 2, we summarize the dHvA experimental situation in LaB_6 and CeB_6. Section 3 contains the details of the band theoretical calculation. Section 4 gives the results of both the f-core and the f-band calculations. The band structure, the description of the Fermi surface and the dHvA frequencies are presented here. In section 5, we compare the theoretical results with dHvA experiments. An analysis of the polarization of the Fermi surface is also included. In section 6, we comment on the calculated momentum density and that obtained from 2D ACAR experiments.

2. dHvA results in LaB_6 and CeB_6

The Fermi surface of CeB_6 has been well studied by the dHvA effect by several groups in the past. One important result which emerged from all this work is its close resemblance with LaB_6. The observed frequencies of CeB_6 are being interpreted therefore using the Fermi surface model of LaB_6 [6]. Hence, it would be useful to briefly summarize here the situation in LaB_6.

The α branch, consisting of $\alpha 1$, $\alpha 2$ and $\alpha 3$, gives a frequency of the order of 10^7 G. They are prominent in most of the (010) and (110) planes but disappear at certain angles. Around this frequency range there are also frequencies labelled β and γ, observed only in

a small angular region. The lower frequencies, of the order of 10^6 G, which are labelled ε, δ and ζ are observed again in a small angular region {100} and {110} planes. There are also frequencies higher than 10^8 G observed, which are labelled μ, ν, λ and ξ [14, 15]. Finally, there are the lowest-frequency (ρ branches), of the order of 10^4 G, which show considerable variation over the field angle in the {100} and {110} planes [14].

The observed frequencies in LaB_6 are interpreted with the Fermi surface model consisting of nearly spherical ellipsoids centred at X connected by necks intersecting the Γ–M axis with small electron ellipsoids along Γ–M. The alpha branch consisting of $\alpha 1$, $\alpha 2$ and $\alpha 3$ arises from three equivalent spherical pieces of Fermi surface centred at the X point, and the γ and ε frequencies from the hole orbits circulating inside the multiply connected ellipsoids centred at M and Γ. The observed dHvA frequencies in PrB_6 and CeB_6 have been interpreted using the above model for LaB_6 [6].

One of the earliest Fermi surface calculations of LaB_6 was performed by Hasegawa and Yanase [16] using the symmetrized non-relativistic self-consistent APW method. The one-electron potential in their calculation is based on the Xα method and the calculations were performed for two different values of the exchange parameter, $\alpha = 2/3$ and 1. The Fermi surface consists of balls located at X points connected by necks along the Γ–M axis. This confirmed the proposed Fermi surface model [14, 15]. In their calculation the necks are short and thick and even if the Fermi energy is displaced the shape is not changed. With this Fermi surface, though they could explain the main branches, in particular the frequencies $\alpha 3$, γ and ε, the overall agreement is not very good. The disagreement with the experiment remained even with a change in the exchange parameter.

The interpretation in which the low-frequency ρ orbits which were initially assigned to the necks was later found to be inadequate. Harima *et al* [17] interpreted these orbits as arising from small flat electron pockets centred at neck positions. These pockets were obtained from the LDA band structure calculations by displacing the 4f level upwards by as much as 100 mRyd.

van Deursen *et al* [3] first studied the Fermi surface of CeB_6 and found the main features of CeB_6 are similar to LaB_6, indicating the 4f electron is almost localized. Onuki *et al* [6] continued the investigation of the Fermi surface in fields up to 14 T and temperatures down to 20 mK. They detected the $\alpha 3$ branch in the limited angular region of 0–45° in the {110} plane and 0–35° in the {100} plane, which is measured from the ⟨100⟩ direction to ⟨110⟩, while van Deursen *et al* [3] observed it throughout the {100} plane. Moreover, they observed the $\alpha 1$ and $\alpha 2$ in a narrow angular region in the {100} plane; this is presumed to be due to magnetic breakdown. These are not observed by Onuki *et al* [6] except at an orientation of ⟨110⟩ which corresponds to $\alpha 1$ of van Deursen *et al* [3]. In addition to observing the main α branch they also found the ρ branch and thus, comparing this with that of LaB_6, they confirmed the existence of an electron pocket in CeB_6, which has been shown to exist in LaB_6.

Besides the main α orbits and the ρ orbits there are several other frequencies in CeB_6 which are centred at ⟨100⟩, ⟨110⟩ and ⟨111⟩ directions. Among them, two branches centred at ⟨100⟩ are thought to correspond to the γ and ε branches of LaB_6, arising from hole-like orbits circulating inside the multiply connected ellipsoids. The cross sectional areas of these orbits depend on the size of the neck.

It was suggested [6] that there were frequencies with heavier mass undetected in dHvA experiments as there was a discrepancy between the quasi-particle mass obtained from dHvA experiments and the thermodynamic mass deduced from specific heat, but recent analysis [7] has confirmed that this is not so. By modelling the Fermi surface sheets for a more general case of prolate ellipsoids of revolution, instead of the spherical approximation

considered earlier, the effective mass was obtained in agreement with that inferred from specific heat.

A detailed calculation of the dependence of the frequencies on the orientation of the magnetic field is needed to confirm the Fermi surface model *assumed* for CeB_6. Though the major features of the Fermi surface such as the X-centred ellipsoids were confirmed by previous calculations, the detailed shape of the Fermi surface is not clear. In the following sections we present the Fermi surface and the dHvA frequencies obtained from our band calculations.

3. Details of the calculation

CeB_6 crystallizes in the cubic $CeBa_6$ structure. The atomic arrangement may be described in terms of the space group $Pm3m$ using its special positions: Ce at the (1a) site (0,0,0) and B at the (6f) sites $\pm(1/2, 1/2, u; 1/2, u, 1/2; u, 1/2, 1/2)$ with $u = 0.207$ and a lattice constant of 7.825 au [25]. We use the fully relativistic spin-polarized linear muffin-tin orbital (SPRLMTO) method [18] where the spin-polarized Dirac equation is solved within the relativistic local spin density functional theory. The valence states include $4f^1$, $5d^1$ and $6s^2$ of Ce and $2s^2$ and $2p^1$ of B. The Ce 5p electrons were treated as part of the core. The unscreened muffin-tin orbitals include s, p, d and f states on Ce (ASA radius 4.040 au) and s and p states of B (ASA radius 2.006 au). For the f-core calculations where the $4f^1$ electron is part of the Ce core, we use only s, p, and d muffin-tin orbitals. The ferromagnetic calculations have been performed for the moments aligned along the c axis and in this case the symmetry is reduced from cubic to tetragonal. For the self-consistent calculations 252 k points were used in the irreducible wedge of the tetragonal Brillouin zone. However, for calculation of the Fermi surface and dHvA frequencies a denser k mesh of 4851 k points in the irreducible wedge (1/16th of the Brillouin zone) was used. Also, the same mesh was used in the calculation of momentum densities.

4. Results

4.1. f-band calculations

With the f electron included as a valence electron, the fully relativistic spin-polarized calculations converge to a stable magnetic state with the spin magnetic moment of $0.94\mu_B$ and the orbital moment $-1.06\mu_B$. The stabilization energy for the magnetic state however is very small, namely 3 mRyd.

Figure 1 shows the band structure of CeB_6 (fully relativistic) along the symmetry directions of the tetragonal Brillouin zone in the magnetic state. The degeneracy of the up and down spin bands is lifted due to spin–orbit coupling, which is clearly seen at the point A in figure 1, where there are the two sets of up and down spin Ce f bands.

As we can see in figure 1, there are four bands which cross the Fermi energy. The lower two bands at the M point (bands 21 and 22), which are broad, correspond to those bands at the Fermi energy in LaB_6. It is a hybridized band of Ce d states and B p states with a little mixture of Ce f states near E_F. The third and fourth bands at the M point (bands 23 and 24), which are flat, are mostly of Ce f character with a small mixture of B p states.

The density of states at the Fermi energy is 11.096 states eV^{-1}/unit cell. Using this one can obtain the specific heat coefficient as

$$\gamma = [(\pi k_B)^2/3]N(E_F).$$

Comparing this with the experimental γ (250 mJ mol^{-1} K^{-2}) one can obtain the mass enhancement as

$$m_{exp}/m_{theory} = \gamma_{exp}/\gamma_{theory}.$$

The values are tabulated in table 1. The values for f band are comparable to those found in other heavy-fermion systems [10, 19, 20] while those for f core seem to be unusually large.

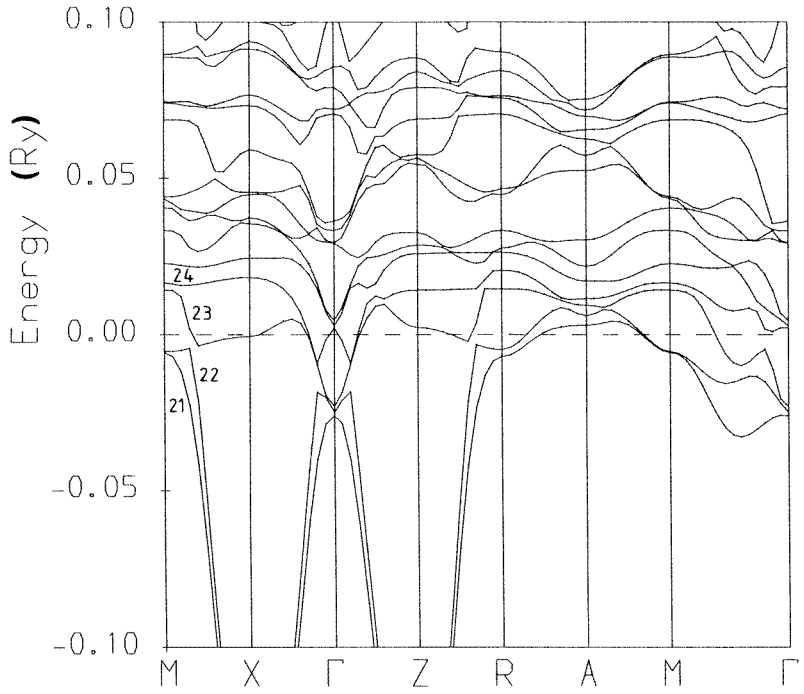

Figure 1. The spin-polarized relativistic band structure of CeB_6 with the f electron treated as valence.

Table 1. The density of states, specific heat coefficient and mass enhancement for CeB_6, in the f-core and f-band cases.

	$N(E_F)$ (states eV^{-1}/cell)	γ (mJ mol^{-1} K^{-2})	m_{exp}/m_{theory}
f-band	11.1	26.12	9.57
f-core	0.61	1.43	174.7

Figure 2 shows the density of states (dos). The vertical line at 0.0 Ryd marks the Fermi energy. The density of states at the Fermi energy is dominated by the Ce f contribution of 92%. The sharp peak centred at -1.1 Ryd consists mainly of B s states. The double-peak structure extending between -0.8 and -0.3 Ryd has mainly B p states hybridizing strongly with s states with a small mixing of Ce s, p and d states. The peak structure near E_F is almost all Ce f states with 92% of the dos at E_F from Ce f states (of up spin), with a small contribution from Ce d states and B p states. This is separated from the one above

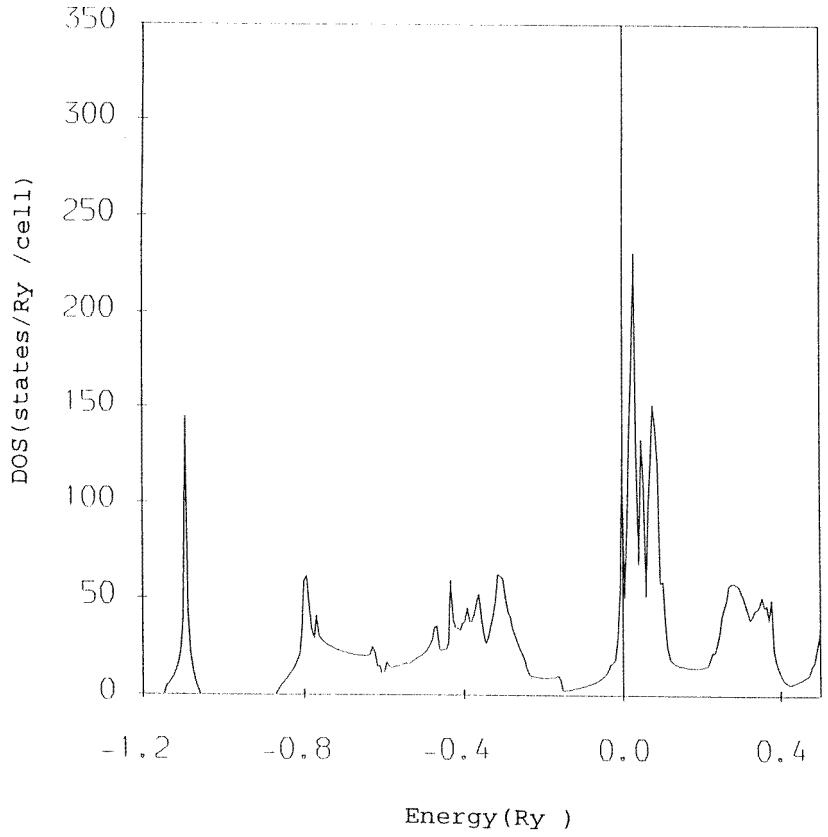

Figure 2. The total dos of CeB_6 with the f electron treated as valence in states Ryd^{-1} cell.

it, centred at 0.3 Ryd, made up of Ce d states. This is different from a scalar relativistic calculation. First of all, the peak structure near E_F is much broadened from 0.07 Ryd without spin–orbit interaction, by almost 100%, to 0.13 Ryd in a relativistic calculation, increasing the dos at E_F. In a relativistic calculation this consists of admixtures of Ce up and down states while in the case of a scalar relativistic calculation the Ce up states at E_F are separated from Ce down states. Thus the Fermi surface is only partially spin polarized in a relativistic approach because of significant hybridization between the up and down spin bands while in a scalar relativistic calculation the Fermi surface will be predominantly of one spin character.

The calculations have also been performed by including the 'combined corrections' [21] and we do not find any significant changes to the Fermi surface. The results reported here are without the combined corrections.

Figure 3 shows the different sheets of the Fermi surface obtained from our f-band calculations. The third band (band 23), which gives about 61% of the contribution to the dos at the Fermi energy, forms the main piece of the Fermi surface, the X-centred 'ellipsoidal' orbits (figure 3). They are not closed perfect ellipsoids as in the case of LaB_6 but are open. Moreover, since the symmetry is reduced from cubic to tetragonal in our calculations where the magnetic moment is aligned along the z axis, the surface centred at

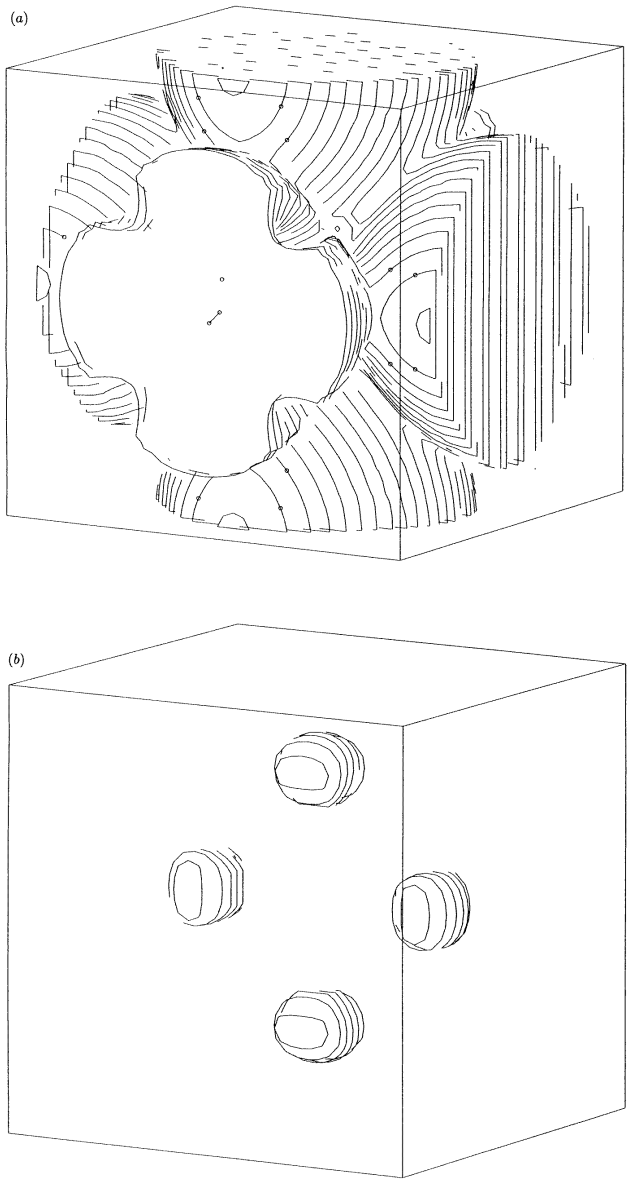

Figure 3. The different sheets of the Fermi surface in the f-band case formed by (*a*), (*b*) band 23 (*c*) band 21 (*d*) band 22 and (*e*) band 24.

Z (001) is a multiply connected surface, different from the other two centred at (100) and (010). These ellipsoids are connected by necks along ⟨110⟩ directions similar to the case of LaB_6. Separated from the main sheets are four small surfaces centred at off-symmetry positions situated along Γ–X and Γ–Y at ($\pm 0.4, 0, 0$) and at ($0, \pm 0.4, 0$) but there are none along Γ–Z (figure 3(b)). This piece of Fermi surface formed by band 23 is much more

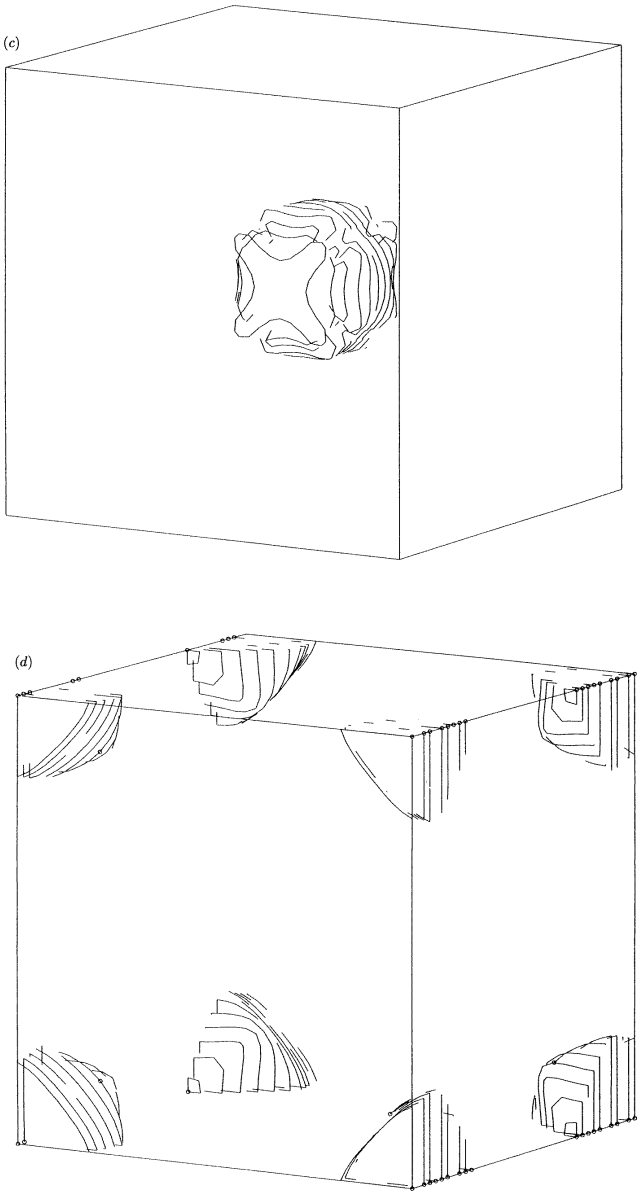

Figure 3. (Continued)

complicated than the simple ellipsoids of LaB_6.

The bands 21 and 22, which are nearly degenerate give rise to more complicated closed large hole surfaces centred at the A point (figures 3(*c*) and 3(*d*)). The bands 22 and 21 contribute about 23% and 14% respectively to the density of states at E_F. These bands, being very flat, are very sensitive to the position of the Fermi energy. A shift in the Fermi energy of 5 mRyd will make the hole orbit of band 21 completely disappear. These bands have mostly f character hybridizing with Boron p, but farther away from E_F they have

(*e*)

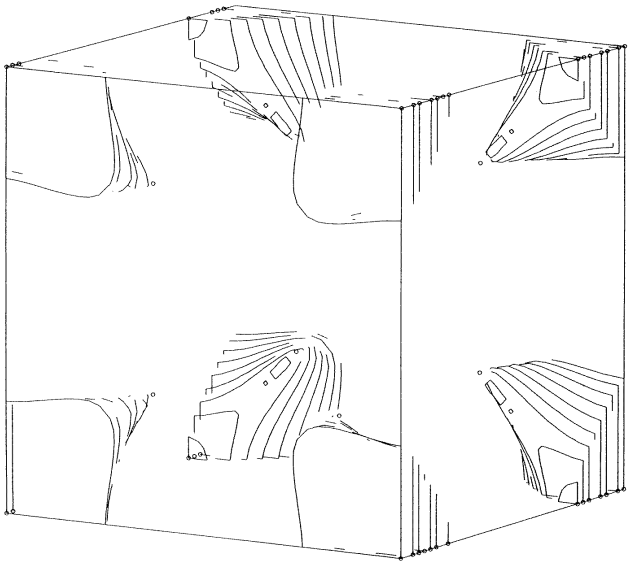

Figure 3. (Continued)

mostly Ce d character.

Finally, the band 24 forms a small closed electron surface centred at the Γ point (figure 3(*e*)). This band contributes only about 2% to the total density of states at E_F.

The dHvA frequency spectrum in the {100} and {110} planes as observed by Onuki *et al* [6] is reproduced in figure 4 and the frequency spectrum calculated from the above Fermi surface sheets is shown in figure 5.

Firstly, the highest-frequency α branch, of the order of 110 MG or 1.1×10^4 T, which remains almost flat in the entire angular region of the {100} plane and part of the {110} plane, arises from the 'ellipsoidal' orbits centred at the X and Y points. They are degenerate in the {110} plane. In the angular region between 50 and 70° in the {110} plane, the frequencies become higher, of the order of 125 MG, this could be the result of the contribution from other sheets and is not included in the figure. The Fermi energy has been shifted upwards by 3 mRyd, which results in a change of the number of electrons by 0.19. The surface centred at Z is more complicated and different from the other two, centred at X and Y, for reasons mentioned earlier, and it was not straightforward to obtain the corresponding frequency. It has not been obtained here.

We assign the next two frequencies below the α branch, which show quite a large dispersion, to γ and ε. They arise from the complicated hole surfaces of the bands 22 and 21 centred at the A point. The band calculations give the hole orbit of the band 22 as too big and we have shifted the Fermi energy upwards by 5 mRyd, which brings down the frequency to just 6×10^3 T in the ⟨011⟩ direction. A further shift of E_F upwards by 1 mRyd changes the frequency to just below 5×10^3 T. For the frequency branch just below this one, which arises from band 21, E_F is shifted upwards by 2 mRyd.

The next frequency, around 2×10^3 T, is named ε'. This arises from the closed electron pocket around the Γ point of band 24. Finally, there is the lowest-frequency branch, given by the small hole pockets of band 23, which are disconnected from the main ellipsoidal sheets

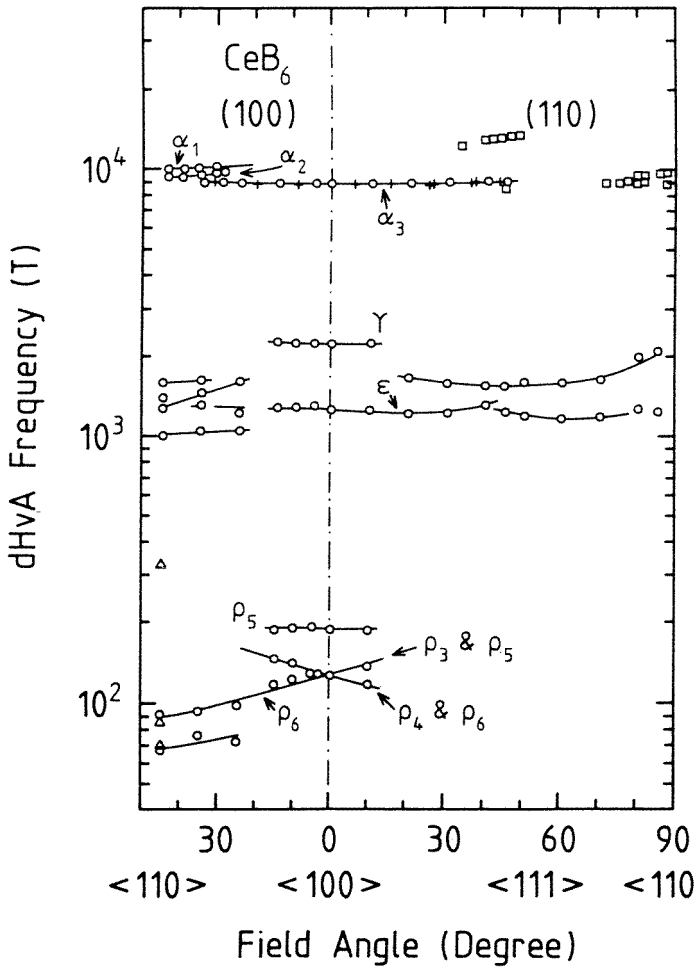

Figure 4. The experimental dHvA frequencies in the {100} and {110} planes as obtained in [6].

and are situated along Γ–X and Γ–Y. These frequencies are degenerate in the {110} plane but they branch off in the {100} plane. Table 2 summarizes the frequencies and the band masses for different orbits along the ⟨100⟩ direction.

4.2. f-core calculations

The non-magnetic band structure of CeB_6 with the f electron as part of the core is shown in figure 6. The calculations are performed first without including the f states in the LMTO basis function. Only one band crosses the Fermi energy giving the density of states at E_F as 0.608 eV^{-1}/cell, a factor of 18.25 smaller than an f-band calculation. At the Fermi energy the d states contribute about 65% of the total; the next highest contribution is from the Boron p states, which is about 34%.

The Fermi surface consists of large 'ellipsoidal' electron orbits centred at the X point. Unlike the f-band case, the system is non-magnetic and so we would restore the cubic symmetry, although the calculations have been done in the tetragonal Brillouin zone. These

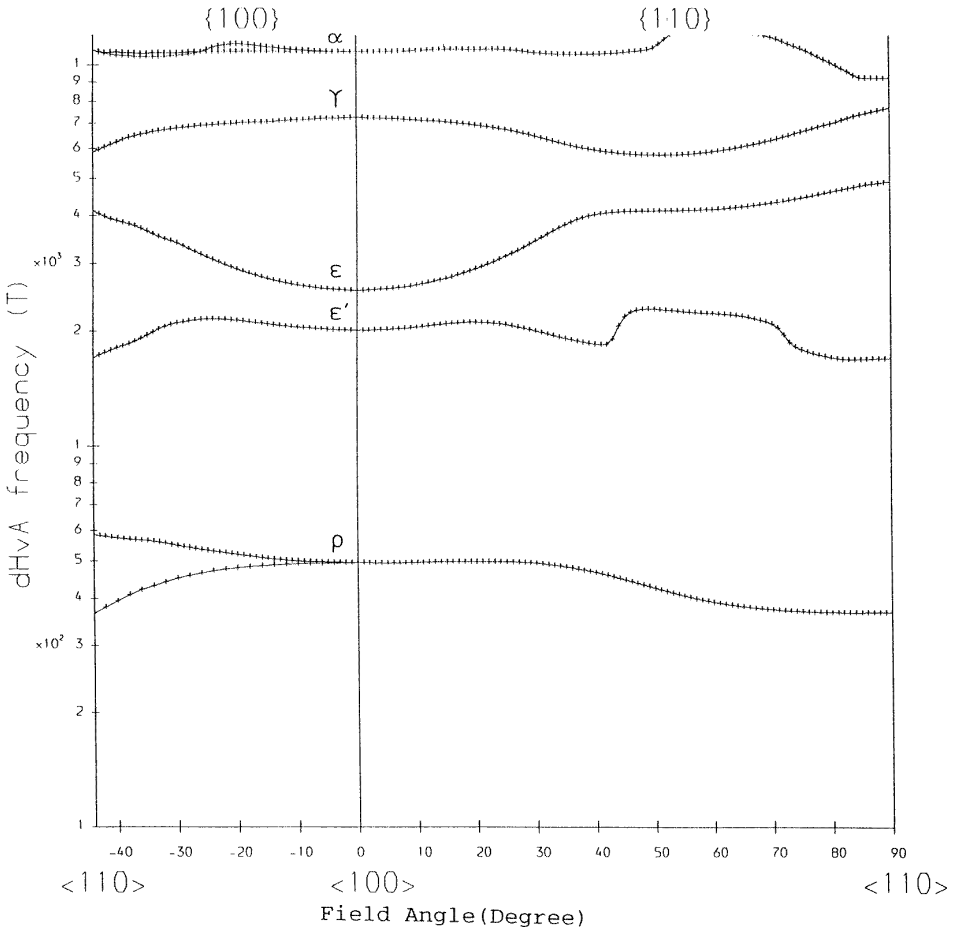

Figure 5. The dHvA frequencies in the {100} and the {110} planes for the f-band case.

'ellipsoids', as in the case of the f band, are open. Consequently they do not form a closed hole orbit centred at the Γ point. Disconnected from this main sheet is a small hole pocket centred at the Γ point. The Fermi surface is different from the Fermi surface of LaB_6, but with a shift in the Fermi level of +20 mRyd one ends up with a Fermi surface topology the same as that of LaB_6.

As a separate calculation, we included the 5f states in the basis set and our results are similar to the case with no f states in the basis set, except that the small hole orbit at the centre appears to be connected with the main sheet, unlike the former case, where it was disconnected from the main sheet. However with a upward shift in the Fermi level it is the same as before. The calculations have also been performed with the core polarized and the band structure remains almost unchanged.

The frequencies obtained in the f-core case with no shift in E_F are shown in figure 7. The highest frequency arises again from the large 'ellipsoidal' electron orbit. The α branch, consisting of two frequencies in the {100} plane, is due to the 'ellipsoids' centred at X and

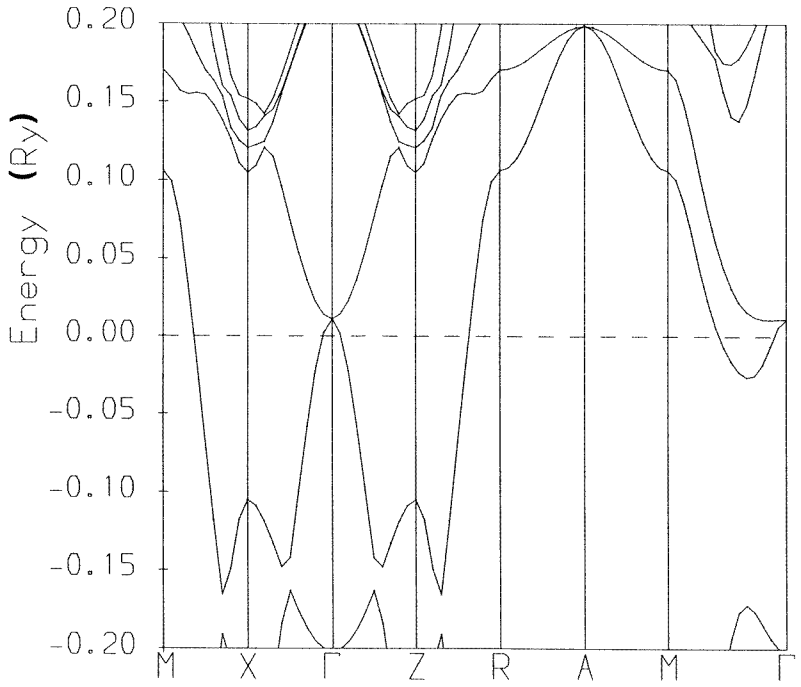

Figure 6. The non-magnetic band structure of CeB_6, treating the f electron as part of the core.

Table 2. The dHvA frequencies and band masses of CeB_6 in the f-band case, for the field along the ⟨001⟩ direction.

	Experiment		Theory		
	F (T)	m^*/m_0	F (T)	m^*/m_0	Band
α	8670	14–21	10 870	5.14	23
γ	2190	15.5	7 278	8.54	22
ε	1300	9.2	2 557	12.33	21
ε'			2 015	1.4	24
ρ	120	3.5	496	2.1	23

Y, and they are degenerate in the {110} plane. The f-core frequencies are slightly less than those of the f-band case but the frequency variation is similar. The next highest frequency (γ branch) arises from the 'ellipsoid' centred at Z, which could be obtained only in a limited angular region. The ε frequency around 4×10^3 T arises from the hole orbit formed by the multiply connected ellipsoids centred at M. The lowest frequency (ρ branch), of the order of 10^2 T, arises from the small Γ-centred hole orbit.

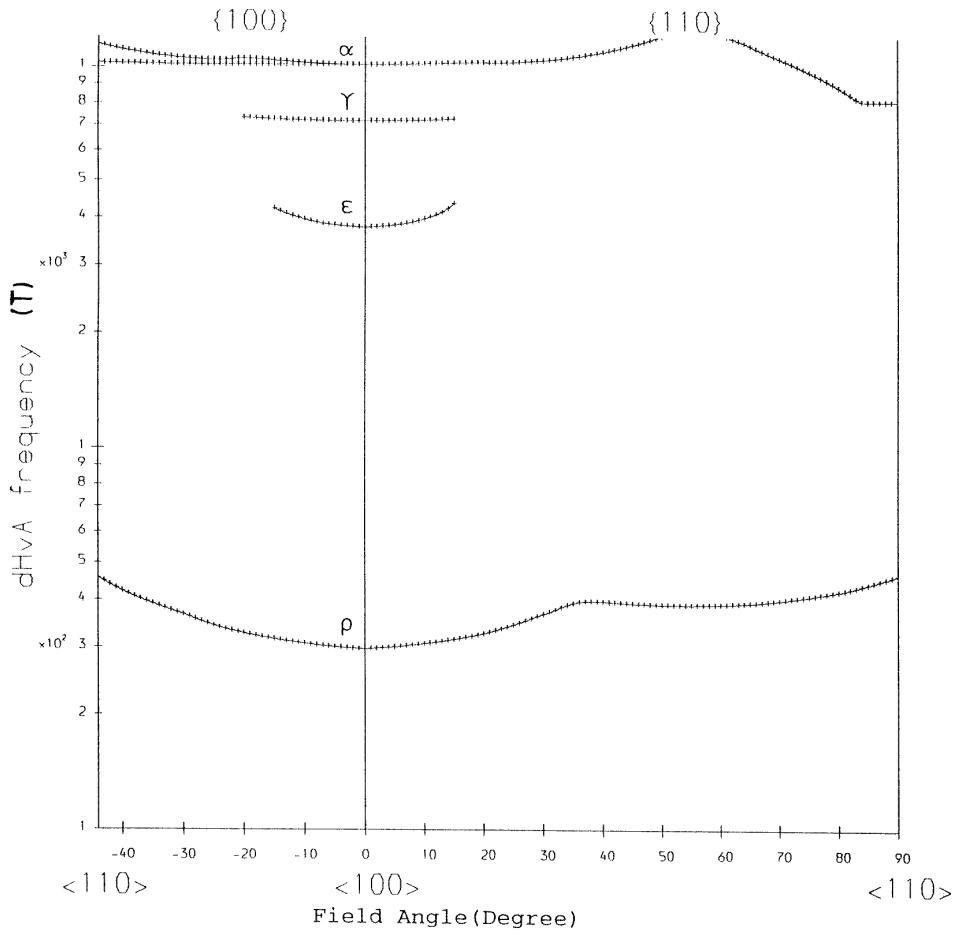

Figure 7. The dHvA frequencies in the {100} and the {110} planes for the f-core case.

5. Discussion

5.1. Frequencies compared with experiment

The highest frequency, i.e., the α branch, is present in all the hexaborides LaB_6, CeB_6 and PrB_6 [6], and originates from the X-centred ellipsoidal orbits, where much attention has been focused. It is interesting to note however that this frequency, which is in agreement with the experiment, is obtained in the calculations, irrespective of whether the f electron is treated as a core electron or as a band electron.

In the f-core case it is the broad d band of Ce hybridizing with B p states which gives rise to this α frequency. This is also true in the case of LaB_6, where the α orbit comes from the broad band consisting mainly of La d states, hybridizing with B p with a little contribution (12%) from La f states. Thus the general band structure features are very similar in LaB_6, CeB_6 (f core) and PrB_6 [9].

Including the f electron as a valence electron in CeB_6 pulls the unoccupied f bands from their high-lying position in LaB_6 to a position just above E_F, thus making the Ce f

contribution to the dos at the Fermi energy as high as 92%. Band 23, which gives rise to the 'ellipsoidal' surface, similar to LaB_6 or CeB_6 (f core) contributing to the α frequency, is essentially of f character.

Thus although the f-core and f-band calculations give rise to similar frequencies, the character of the states at the Fermi energy is completely different. This is revealed in the calculated band masses. In the f-core case, the enhancement over the bare electron mass (m_{band}/m_e) is between 0.23 and 0.42 and it is about 0.5 for LaB_6. In the f-band case, the enhancement ranges between five and eight depending on the orientation of the magnetic field. Though the band masses are enhanced compared to the f core or LaB_6, they are significantly short of the observed enhancement, suggesting that the f electrons are not sufficiently localized. This is a known failure of the LDA when applied to strongly correlated electron systems, where many-body effects are not included. A renormalized band structure [22] or one incorporating self-interaction correction (SIC) [23] would perhaps improve the values for the band masses.

The f-core calculations do not give a satisfactory account of all the frequencies. We obtain too few frequencies to account for all the observed frequencies of CeB_6. The α frequency is obtained in agreement with experiment. We also obtain two frequencies in the middle region, which could be identified with the γ and ρ branches of CeB_6, but in a higher-frequency range. The ρ branch arises from the pocket centred at the Γ point and we obtain only one frequency instead of multiple branches. The topology of the Fermi surface however can be changed to resemble that of LaB_6 by shifting the Fermi level, in which case the ρ branch can be interpreted satisfactorily as similar to that of LaB_6 [17], but still we would fail to account for all the frequencies observed in CeB_6, especially those in the middle region of the frequency spectrum between the α and the ρ branches.

Thus the frequencies in the middle region seem to be more crucial than the α branch or the ρ branch as they are the ones which mainly make the frequency spectrum of CeB_6 different from that of LaB_6. These are now the orbitals which will be reinvestigated in detail [27].

In the f-band case we do obtain additional frequencies in the middle region in comparison to the f-core case. Experimentally, in the frequency range between 10^3 and 2×10^3 T one sees two or three frequencies, depending on the direction. There are the γ and the ε branches, which are continuous up to 15° in the {100} and in the {110} planes, similar to what is observed in LaB_6. There are also other frequencies in this range between τ and ε, continuous in both the {110} plane and the {100} plane.

In our case, there are three frequencies in the range between 10^3 and 7×10^3 T. The γ and the ε branches are in a higher range than what is observed. For the γ and the ε frequencies which originate from the hole orbits centred at the A point formed by bands 21 and 22, the band masses are between seven and nine times the bare electron mass. This high value for the band mass is due to the fact that these bands are flatter, giving rise to big hole orbits at the A point, resulting in higher frequencies and higher band masses. For the frequency branch below these (ε' branch) from the Γ-centred electron orbit the masses are in the range between one and three which is also true for the ρ branch.

The lowest-frequency ρ branch in our calculations is again higher compared to the experimental values in both the f-band and f-core calculations. In the f-band case, these arise from the small hole pockets along Γ–X and Γ–Y as shown in figure 3(*b*). This interpretation of the ρ branch is different from the earlier one based on the Fermi surface of LaB_6 in which case it is due to the existence of ellipsoidal electron pockets along $\langle 110 \rangle$ [17].

In summary, the f-band calculations are not satisfactory either. This is particularly

true for the frequencies ε and γ, characterized by large f–d hybridization, which appear much higher than what is observed. Moreover, the ρ branch, which is observed to be non-degenerate in {110}, appears degenerate in our calculations. One possible explanation for the discrepancies may be the fact that the calculations are performed for a specific direction of the magnetic field, namely the z axis, which makes the system have tetragonal symmetry. This may not correspond to the magnetic structure in which the experiments are performed. A different magnetic structure would change the conduction-electron–f-electron hybridization, thus affecting the topology of the bands and hence the frequencies. The polarization of the Fermi surface will also be affected.

5.2. Spin polarization of the Fermi surface

In the present calculations, the total spin moment is $-0.94\mu_B$ at the calculated value of E_F, indicating a strong polarization at the Fermi energy. To see whether one can change this strong polarization at the Fermi level by a mere shift of E_F, we calculated the spin moment by varying the Fermi energy. This is plotted in figure 8. We see that the spin polarization does remain strong and it is inherent in the band structure.

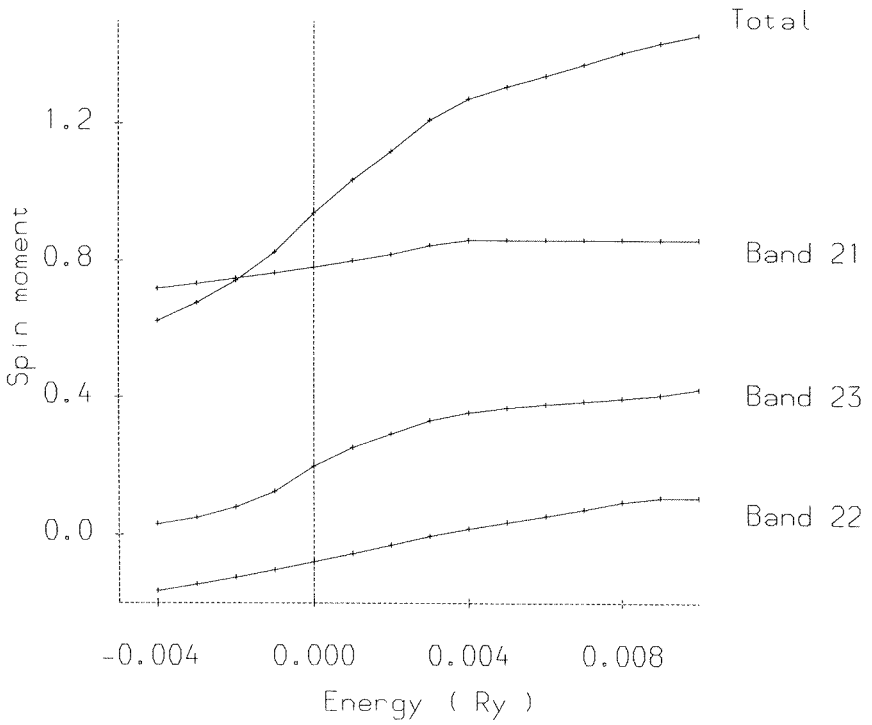

Figure 8. The total spin moment and spin moment in μ_B from individual bands for different values of the Fermi energy.

To see to what extent each sheet of the Fermi surface is polarized in the present calculations, we plotted, in figure 8, the spin polarization of each of those bands which

occur at the Fermi energy separately. The four bands have very different behaviour in their spin polarization. Band 24 is not included as its contribution to the density of states in the energy range considered here is very little. We find that band 23, which forms the biggest piece of the Fermi surface, giving rise to the α branch, is not as heavily polarized as band 21. It disperses from about 10 mRyd below E_F to about 14 mRyd above E_F, and the spin polarization varies from almost zero at 4 mRyd below E_F to $0.33\mu_B$ at 3 mRyd above E_F. It carries almost all of the polarization in the f channel and the sharp rise in the total polarization originates from this f contribution.

Bands 21 and 22, which form the A-centred hole orbit, have a considerable contribution to the spin moment from the d channel also. Band 21 gives the biggest contribution to the spin moment at the Fermi surface, of about $0.8\mu_B$, and this remains constant with a shift in E_F. For band 21, the f contribution varies from 66% at 4 mRyd below the calculated E_F to about 71% at 5 mRyd above E_F, and the rest is due to the d channel. The d and f channels add up to enhance the polarization. For band 22, the d contribution is of similar magnitude as for band 21, but in the opposite direction. The f spin moment is only about $0.03\mu_B$ while the d spin moment is $-0.2\mu_B$ at 4 mRyd below E_F, but at 5 mRyd above E_F it increases to $0.23\mu_B$, which is of similar magnitude to the d contribution. However as they are in the opposite directions, the resultant net moment is very small.

The polarization of the α orbit, being only 21% of the total at E_F, is consistent with the experimental finding [7] that the orbit is unpolarized. Thus we have a different interpretation of the data from that of Harrison *et al* [7]. In [7], they used the experimental observation that the α orbit is unpolarized to deduce that the α sheet (and all other sheets) was doubly degenerate. This interpretation left an experimental puzzle as to why no splitting of the α orbit was observed in the high magnetic fields used in the experiments [27]. In our calculations we find that the α orbit is both (essentially) unpolarized and non-degenerate and so would not be expected to show splitting in a magnetic field.

Harrison *et al* [7] used the observed sheets of the Fermi surface with their deduction of double degeneracy to estimate the total number of metallic electrons to confirm their assumption that the Ce f electron is fully localized. This deduction is not necessary as in our calculations the f electron has been treated as a band electron.

5.3. Comparison with 2D ACAR

In this paper, although the main emphasis is on the results of dHvA frequencies, we also calculated the electron occupancies in k space by integrating the Fermi surface obtained in the f-core and in the f-band cases along the [001] direction, so that the results can be compared with the recent 2D angular correlation of electron–positron annihilation radiation [8] experiments in CeB_6. The integrated results were directly convoluted with the experimental resolution [8] so that what we obtain is directly comparable with the experimental results. This, we hoped, would help to provide an unambiguous result about the f-electron contribution to the Fermi surface.

In [8], the authors used a Fermi surface model consisting of nearly symmetrical electron ellipsoids centred at the X points and connected by necks along the Γ–M axes for comparison with their experimental momentum density integrated along the [100] direction, filtered as described in [8]. This Fermi surface model is based on that of LaB_6.

Figure 9(a) shows the experimental filtered projected momentum density for CeB_6 after being LCW [26] folded in the first Brillouin zone (k-space occupancy). Figure 9(b) and 9(c) shows our theoretical results of the f-core calculations without and with shifting of the Fermi level respectively. As we can see figure 9(b) is very different from the experimental filtered

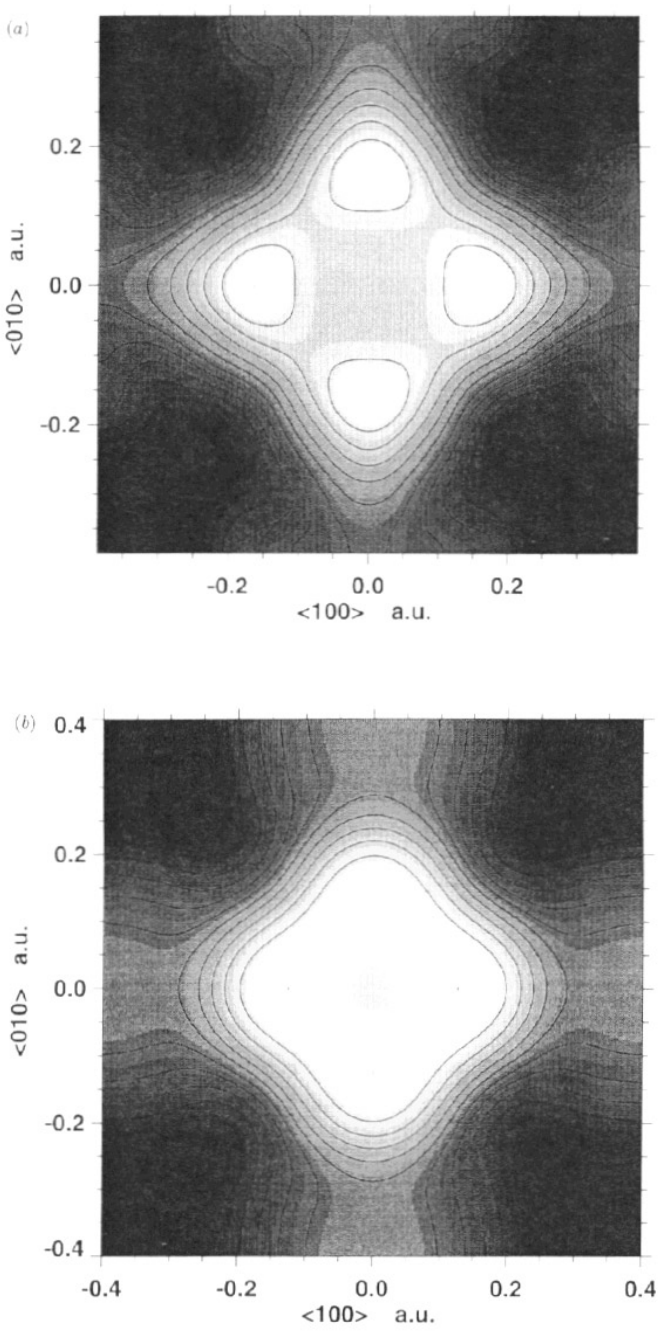

Figure 9. (*a*) The experimental momentum density compared with that obtained from calculations: (*b*), (*c*) f-core calculations with the calculated E_F (0.035 Ryd) and shifted E_F (0.01 Ryd) respectively; (*d*) f-band calculations with adjusted E_F (see the text); (*e*) the contribution from band 23 only. In the grey scale white corresponds to high and dark to low intensity. The spread of intensities of the LCW-folded filtered data is $\sim$ 13 times the average (or 'typical') statistical uncertainty of the intensity.

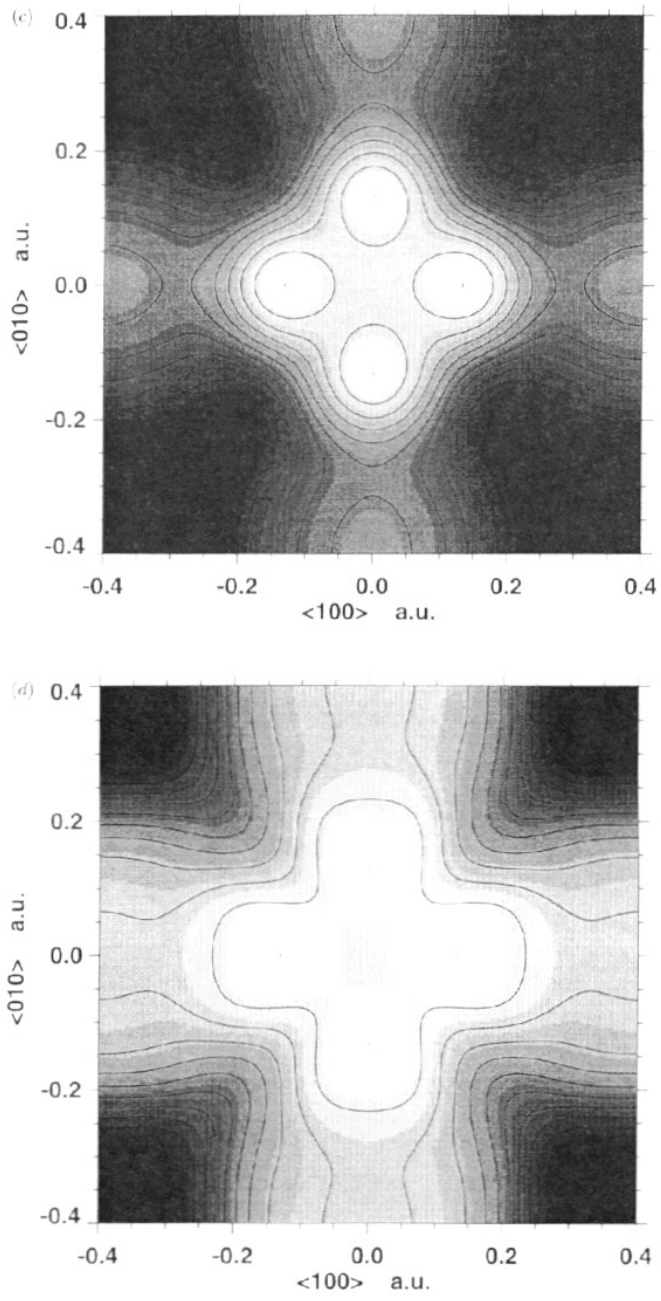

Figure 9. (Continued)

k-space occupancy of CeB_6; by shifting the Fermi energy one obtains closer agreement to the experimental data but the shift in the Fermi level is very large. However, a full comparison between the calculations and the experiments should not be sought since the calculations neglect the electron–positron matrix elements. We should only concentrate on the gross features of agreement.

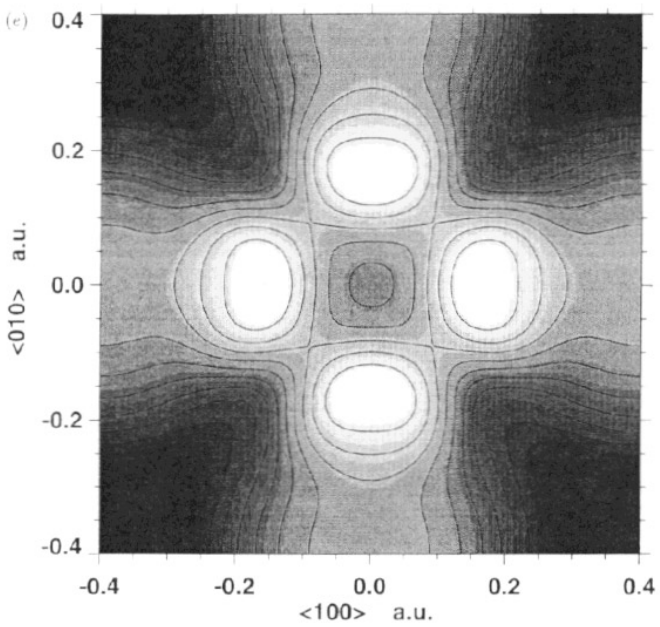

Figure 9. (Continued)

Figure 9(*d*) shows the *k*-space occupancy from the f-band calculations. Here there are four bands involved and the adjustments of Fermi energy for the bands are the same as for the calculation of the dHvA frequencies (refer to subsection 4.1). This does not give a good agreement with the experimental results but compared with the f-core calculations the agreement is better. In contrast to the f-core, the f-band *k*-space occupancy sums over four bands and therefore the neglect of the electron–positron matrix elements might be more severe here, since they could affect each band contribution differently. To investigate this, we calculated the contribution of only band 23 to the *k*-space occupancy. This is shown in figure 9(*e*). This demonstrates that the 2D ACAR experiments probe mostly the contribution of band 23. To further investigate this, one would need to consider the electron–positron matrix elements [24]. Another caveat is that the calculations are performed in the ferromagnetic phase and the experiments are performed at 30 K, where the system will be in the paramagnetic phase, which most probably is a disordered local moment phase.

6. Conclusions

We have performed fully relativistic LMTO calculation of CeB_6 within the LDA, which is an improvement over the previous calculations [9, 13] and calculated the Fermi surface and dHvA frequencies. In the f-band case, the calculations are performed in the simple ferromagnetic structure and not in the antiferroquadrupolar phase in which the dHvA experiments are performed.

The dHvA frequencies obtained from both the f-core and f-band calculations is in agreement with the experiment for the α branch but neither of them give a satisfactory explanation for all the other observed frequencies. The f-band calculations give some additional features in the frequency spectrum. In particular, we conclude that the ε, ε' and

γ frequencies from bands 21 and 22 are due to the f-electron contribution to the Fermi surface. Comparing with the positron annihilation experiments seems to indicate that the contribution of the α sheet dominates the spectrum.

Summarizing, we find the angular dependence of the dHvA frequencies in the f core to be too similar to that of LaB_6 and to miss the additional features seen in CeB_6. Whilst these features can be seen in the f band their detailed frequency spectrum does not have the required agreement with the experiment. Though one can attribute the failure of the f-band model to the LDA, one cannot rule out changes to the calculated dHvA frequencies due to magnetic structure effects.

CeB_6 was originally one of the few heavy-fermion materials in which dHvA data are used with the results from the band theory to deduce that the f electron is localized, but we have shown that this is more subtle and it would be too simplistic to assume that the f-core calculations of CeB_6 would be more appropriate, although similarities exist between the dHvA spectrum of CeB_6 and LaB_6. When spin polarization is taken into account, the experimental data seem to be consistent with the f-band picture. Further experiments to deduce the spin polarization of other orbits are needed to confirm the theoretical picture.

Acknowledgments

We would like to thank Professor M Springford for bringing the problem of CeB_6 to our attention and for his extensive helpful discussions in the comparisons between the experimental and theoretical dHvA frequencies and amplitudes. We would also like to thank Dr A Alam and the rest of the positron group at Bristol for helpful discussions, especially S Dugdale for his help in producing the 3d plots of the Fermi surface. This work was performed while MSB was supported by EPSRC grant GR/J89873.

References

[1] Norman M R, Albers R C, Boring A M and Christensen N E 1988 *Solid State Commun.* **68** 245
[2] Sandratskii L M, Kubler J, Zahn J, Zahn P and Mertig I 1994 *Phys. Rev.* B **50** 15 834
[3] van Deursen A P J, Pols R E, de Vroomen A R and Fisk Z 1985 *Less-Common Met.* **111** 331
[4] Joss W, van Ruitenbeek J M, Crabtree G W, Tholence J L, van Deursen A J P and Fisk Z 1987 *Phys. Rev. Lett.* **59** 1609
[5] Matsui M, Goto T, Kunii S and Sakatsume S 1993 *Physica* B **186** 126
[6] Onuki Y, Komatsubara T, Reinders P H P and Springford M 1989 *J. Phys. Soc. Japan* **58** 3698
[7] Harrison N, Meeson P, Probst P A and Springford M 1993 *J. Phys.: Condens. Matter* **5** 7435
[8] Biasini M, Alam M A, Harima H, Onuki Y, Fretwell H M and West R N 1994 *J. Phys.: Condens. Matter* **6** 7823
[9] Langford H D, Temmerman W M and Gehring G A 1990 *J. Phys.: Condens. Matter* **2** 559
[10] Taillefer L, Floquet J and Lonzarich G G 1991 *Physica* B **169** 257
[11] Suvasini M B, Guo G Y, Temmerman W M and Gehring G A 1993 *Phys. Rev. Lett.* **71** 2983
[12] Effantin J M, Rossot-Mignod J, Burlet P, Bartholin H, Kunii S and Kasuya T 1985 *J. Magn. Magn. Mater.* **47&48** 145
[13] Norman M R and Koelling D D 1993 *Handbook of the Physics and Chemistry of Rare Earths* ed K A Gschneider, L Eyring, G H Lander and G R Choppin (Amsterdam: Elsevier) ch 10
[14] Ishizawa Y, Tanaka T, Bannai E and Kawai S 1977 *J. Phys. Soc. Japan* **42** 112
Ishizawa Y, Nozaki H, Tanaka T and Nakajima T 1980 *J. Phys. Soc. Japan* **48** 1439
[15] Arko A J, Crabtree G, Karim D, Mueller F M, Windmiller L R, Ketterson J B and Fisk Z 1976 *Phys. Rev.* B **13** 5240
[16] Hasegawa A and Yanase A 1977 *J. Phys. F: Met. Phys.* 1977 **7** 1245
[17] Harima H, Sakai O, Kasuya T and Yanase A 1988 *Solid State Commun.* **66** 603
[18] Ebert H 1988 *Phys. Rev.* B **38** 9391
[19] Takegahara K, Harima H and Kasuya T 1985 *J. Magn. Magn. Mater.* **47&48** 263

[20] Harima H and Yanase A 1991 *J. Phys. Soc. Japan* **60** 21
[21] Skriver H L 1984 *The LMTO Method* (Berlin: Springer)
[22] Zwicknagl G 1992 *Adv. Phys.* **41** 203
[23] Temmerman W M, Szotek Z and Winter H 1993 *Phys. Rev.* B **47** 1184
[24] Rozing G J, Mijnarends P E and Koelling D D 1991 *Phys. Rev.* B **43** 9515
Rozing G J, Mijnarends P E and de Chatel P F 1991 *Phys. Rev.* B **43** 9523
Kubo Y and Asano S 1989 *Phys. Rev.* B **39** 8822
[25] Blum P and Bertaut F 1954 *Acta Crystallogr.* **7** 81
[26] Lock D G, Crisp V H and West R N 1973 *J. Phys. F: Met. Phys.* **3** 561
[27] Springford M 1995 private communication